J Nanostruct 16(4): 4717-4727, Autumn 2026

RESEARCH PAPER

Green Selenium Nanocomposite Loaded with Ampicillin: Synthesis, Characterization, and Synergistic Antibacterial Activity Against Isolates from Prostate Cancer Patients

*Malik Ahmed A. Al-Yassari *, Kaisar Abdul Sajjad M. Hussein*

Department of Biology, College of Science, University of Kerbala, Iraq

ARTICLE INFO

Article History:
Received 02 May 2026
Accepted 16 July 2026
Published 01 October 2026

Keywords:
Ampicillin-loaded nanocomposite
Green synthesis
Multidrug-resistant bacteria
Selenium nanoparticles
Synergistic antibacterial activity

ABSTRACT

This study aimed to prepare green selenium nanoparticles (SeNPs) using ashwagandha root extract, then load them with the antibiotic ampicillin (Amp-SeNPs) to improve its pharmaceutical properties and evaluate its synergistic inhibitory activity against resistant bacterial strains isolated from prostate cancer patients with urinary tract infections. Characterization techniques (FTIR, AFM, SEM) confirmed the success of the green synthesis, showing spherical nanoparticles with an average size of 106 nm before loading, which increased to 118 nm after loading, along with significant increases in surface roughness and root mean square height, confirming antibiotic conjugation. The study included three bacterial isolates: E. coli, K. pneumoniae, and P. aeruginosa. The inhibitory activity evaluation showed that the loaded nanocomposite (Amp-SeNPs) exhibited significant differences ($P \leq 0.05$) compared to the antibiotic or nanoparticles alone. The inhibition zone diameter against E. coli was 24.63±1.36 mm, compared to 1.25±0.366 mm for ampicillin alone and 11.88±1.74 mm for SeNPs alone. At the higher concentration, inhibition reached 27.50–27.75 mm for all three species, along with a marked reduction in MIC values.

How to cite this article
Ahmed A. Al-Yassari M, Abdul Sajjad M. Hussein K. Green Selenium Nanocomposite Loaded with Ampicillin: Synthesis, Characterization, and Synergistic Antibacterial Activity Against Isolates from Prostate Cancer Patients. J Nanostruct, 2026; 16(4):4717-4727. DOI: 10.22052/JNS.2026.04.021

INTRODUCTION

Prostate cancer is one of the most common cancers among men worldwide [1]. Prostate cancer treatments suppress the immune system, making patients more susceptible to opportunistic bacterial infections, particularly in the urinary tract [2]. Multidrug resistance (MDR) among bacteria poses a growing global health challenge. This phenomenon leads to the failure of traditional antibiotic treatment lines such as ampicillin and increases mortality and morbidity rates among patients [3]. In this field, nanotechnology has emerged as a highly effective solution to this problem by addressing the antibiotic resistance crisis [4]. Researchers have focused on nanoparticles due to their unique biological properties. However, some drawbacks have emerged with chemically prepared nanoparticles, especially those used in vivo, due to their high toxicity and metabolic interference. Therefore, research has focused on safer alternatives, including the preparation of nanoparticles using green methods [5]. Preparing these particles using plant extracts is a safer, less expensive, and more environmentally friendly alternative compared to chemical and physical methods that consume

* *Corresponding Author Email: malik.aboud@s.uokerbala.edu.iq*

high energy [6]. Loading nanoparticle-antibiotic conjugates with conventional antibiotics reveals a potential synergistic strategy [7]. Loading biologics onto the surface of selenium nanoparticles increases their local concentration at the bacterial cell wall, enhancing their antibacterial stability and facilitating their penetration of cellular resistance mechanisms [8]. Bacterial species such as Escherichia coli, Klebsiella pneumoniae, and Pseudomonas aeruginosa are among the most common gram-negative bacilli in the gastrointestinal tract that cause bacterial prostatitis. Escherichia coli is the most common cause of bacterial prostatitis worldwide. In certain cases, the mechanism of bacterial prostatitis reflects the ascent of pathogens from the urethra to the prostate by the reflux of infected urine into the prostatic ducts if predisposing factors such as urinary tract infections, bladder outlet obstruction, and urological procedures that penetrate the prostate's natural defenses are present [9].

MATERIALS AND METHODS

Preparation of the aqueous extract of the Ashwagandha plant1-3

The roots of the Ashwagandha plant (Withania somnifera) were thoroughly washed with distilled water to remove impurities and dirt. They were

Fig. 1. Ashwagandha plant roots.

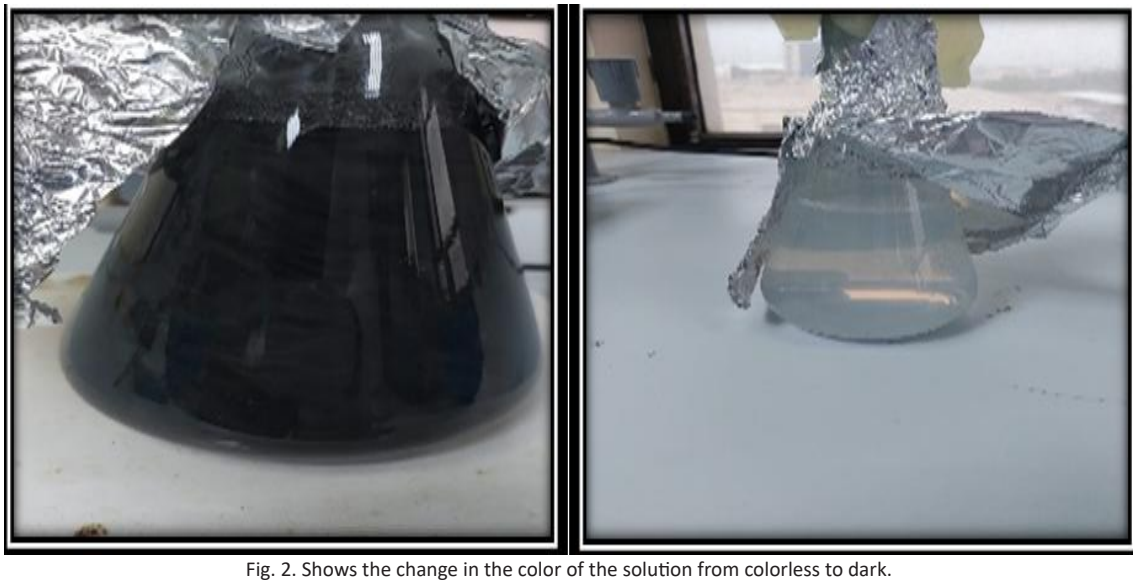

Fig. 2. Shows the change in the color of the solution from colorless to dark.

then dried in the shade and ground into a fine powder. Ten grams of the powder were weighed and added to 100 ml of sterile distilled water in a conical flask. The mixture was then heated at 80°C for 30 minutes with continuous stirring and allowed to cool. The solution was then filtered using Whatman No. 1 filter paper to obtain a clear and pure extract. The extract was then stored in a refrigerator at 8°C until use as shown in Fig. 1. [10,11].

Green preparation of selenium nanoparticles (SeNPs):2-3

A sodium selenite (Na_2SeO_3) solution is prepared at a concentration of 10–50 mM in distilled water. This solution is then added to ashwagandha extract at a specific volumetric ratio (2:8) under continuous magnetic stirring at 80°C. The process reduces selenium ions and forms nanoparticles, causing the solution to change color from colorless to dark as shown in Fig. 2 [12].

Loading the nanocomposite with the antibiotic ampicillin (Amp-SeNPs)

Weigh 5 mg of the antibiotic under study and add 2 ml of distilled water (Solution No. 1). Take 250 mg of selenium nanoparticles in 40-50 ml of deionized distilled water (Solution No. 2). Using

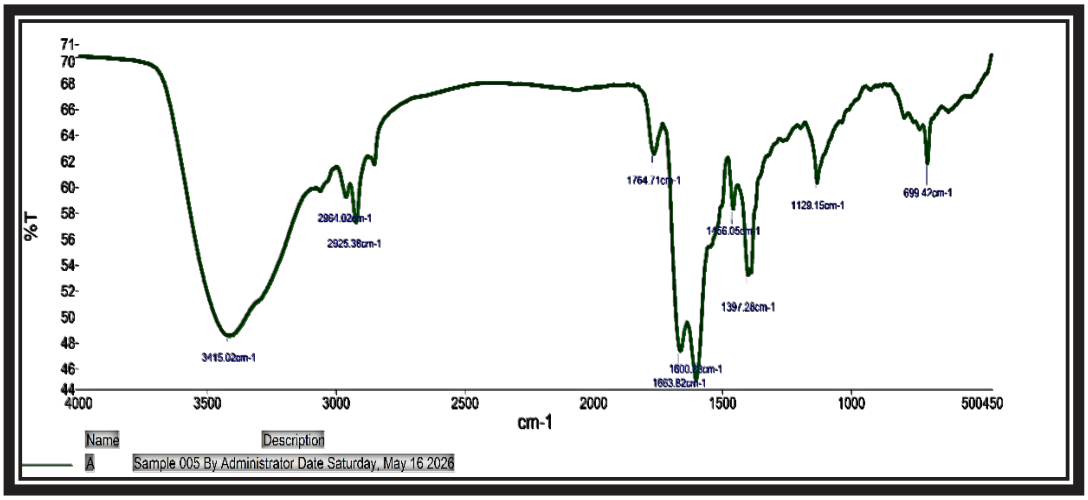

Fig. 3. FT-IR infrared spectrum of the antibiotic-loaded nanocomposite (Amp-SeNPs).

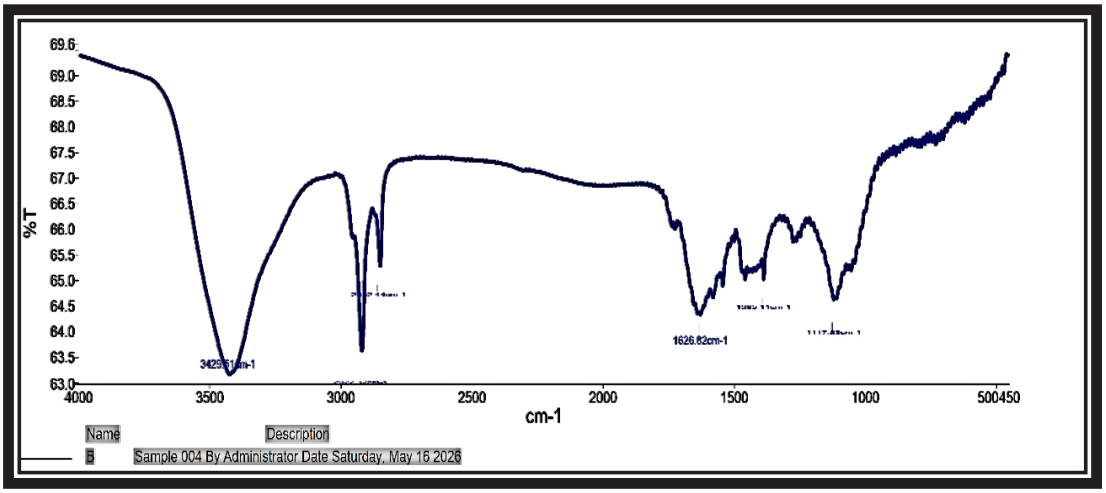

Fig. 4. FT-IR infrared spectrum of free nanocomposites (SeNPs).

a hypersonic bath, add Solution No. 1 to Solution No. 2 in the water bath and leave for 5 minutes. Transfer to a heated shaking plate at 60°C and pH 6-6.5 to bring the total volume to 50 ml. Leave the mixture under continuous stirring for 24 hours in the dark to ensure physical adsorption or chemical bonding between the active groups of the antibiotic and the nanoparticles, until one-third of the solution is reached (Solution No. 3). Then wash the precipitate with distilled water and pass the third solution through a 220-400 mesh filter to remove any lumps. Finally, dry to obtain a pure nano powder for subsequent use in treating isolated bacteria with the minimum inhibitory concentration of both the antibiotic and the nanoparticle compound [13,14].

Prepare the minimum inhibitory concentration for both the compound and the synergistic antagonist

5 mg of the antibiotic was dissolved in 2 mg of distilled water to obtain 0.0025 mg of the antibiotic with the prepared volume of the nanocomposite. Two concentrations of 64-32 micrograms of the antibiotic were taken with 128-64 micrograms of the nanocomposite, and the isolated bacterial species were treated with 50 microliters of each concentration [15].

Characterization Techniques for Nanomedicine

The nanocomposite is characterized by Fourier transform infrared spectroscopy (FTIR), scanning electron microscopy (SEM), and atomic force microscopy (AFM) [16,14].

Evaluation of the inhibitory effect against bacterial strains

A bacterial suspension was prepared for each bacterial species according to the McFarland scale (0.5 McFarland). The bacteria were spread on Müller-Hinton Agar plates. Spreading was done by drilling with a cork drill into the agar, and the bacteria under study were treated with pre-prepared concentrations [17,18].

RESULTS AND DISCUSSION

Characterization of nanocomposites (SeNPs)

FT-IR Infrared Spectrum

The infrared spectrum was studied to characterize the prepared selenium nanocomposite loaded with the antibiotic ampicillin.

FT-IR infrared spectrum of the antibiotic Ampicillin loaded onto green selenium nanoparticles (SeNPs)

The FTIR analysis results of the antibiotic-loaded nanocomposite (Amp-SeNPs) (Fig. 3) showed the emergence of a transverse absorption band displaced at 3415.02 cm^{-1} from its position in the free antibiotic and the free nanocomposite, which recorded frequencies of 3429.51 and 3297.70 cm^{-1}, respectively. These shifts are attributed to the vibrations of the hydroxyl group (O-H) and the aromatic H-C groups. The frequencies recorded in the antibiotic and the nanocomposite (2062.40 and 2852.44 cm^{-1}, respectively) indicated

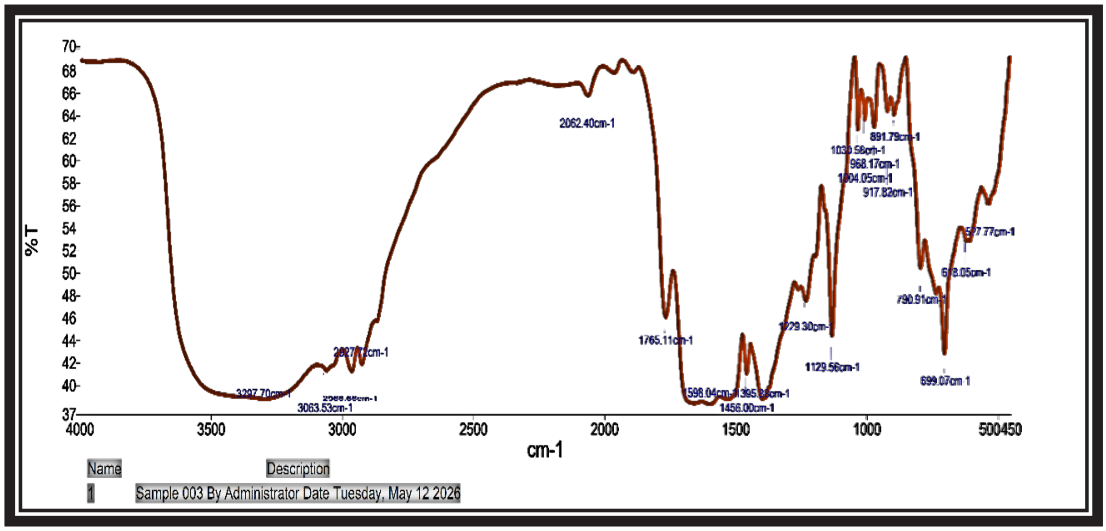

Fig. 5. FT-IR infrared spectrum of the free antibiotic (AMP).

new displacement sites and the riding of the amine group (N-H) bond towards the prepared nanocomposite, appearing at frequencies of 2964.02 and 2925.38 cm^{-1}. Subsequently, a sharp peak appeared at a frequency of 1764.71 cm^{-1}, attributed to the displaced C=O bond of the superposition of carboxylic acids and ketones. Aldehydes, and as we note, the frequency of the beam's mounting within the 1637.40 cm^{-1} site remained almost at the same level, and the appearance of the waves (1456.05, 1397.28, 1129.15) cm^{-1} clearly indicates the association of the antibody molecules with the nanocomposite. The study results also indicated that the presence of absorption at the wave (699.42) cm-1 differed from what was recorded by the wave in Figs. 4 and 5, which appeared (1117.83, 527.77) cm-1 towards the prepared nanocomposite, indicating the success of the loading of the Wincen cavate and the diffusion of the treatment molecules within the molecules of the prepared nanocomposite [17].

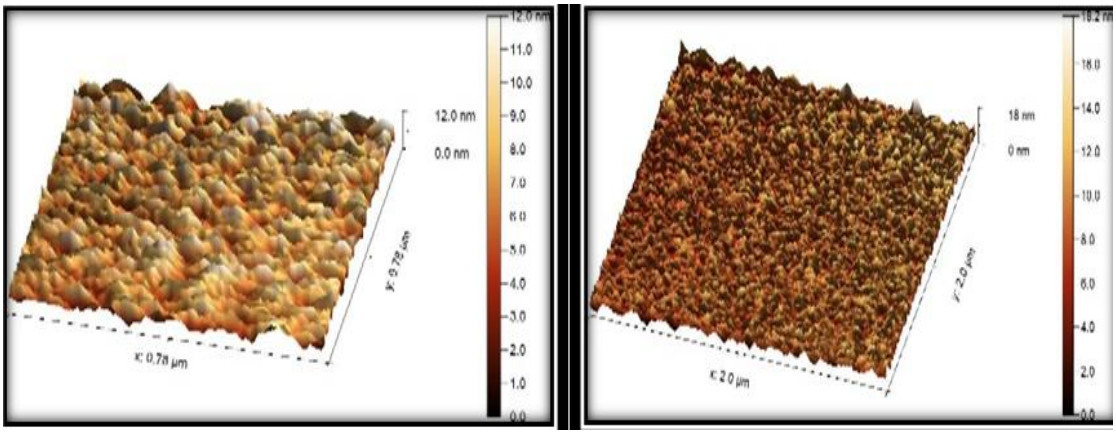

Fig. 6. Atomic Force Microscope image of the (SeNPs) nanocomposite showing the highest peak height and surface shape before loading with the antibiotic (AMP).

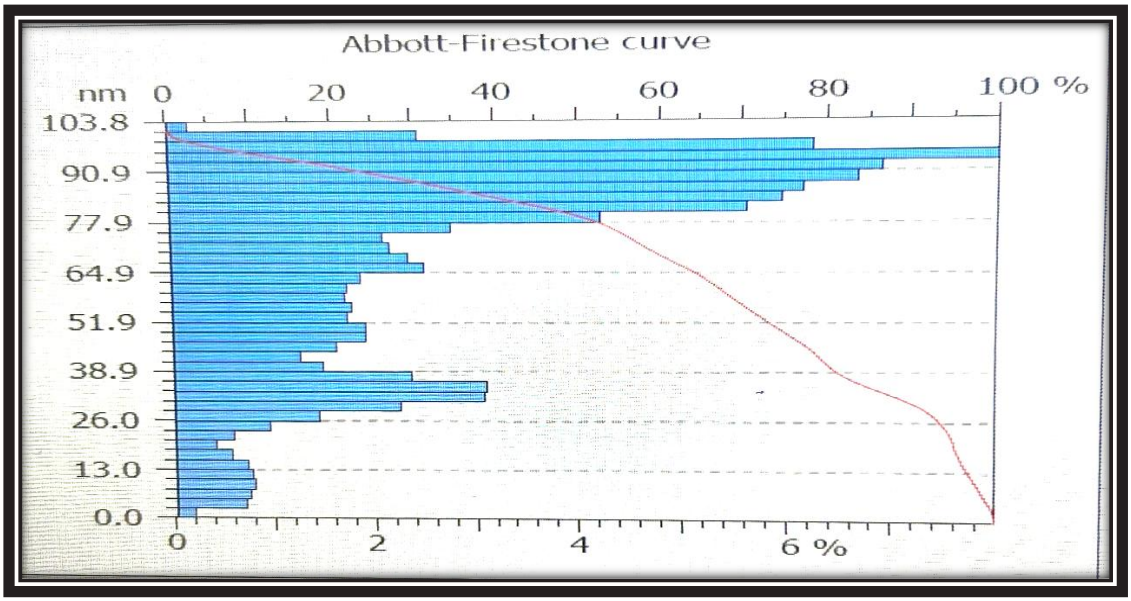

Fig. 7. Shows the particle size distribution of the nanocomposite (SeNPs) before loading with the antibiotic (AMP).

Atomic force microscopy (AFM) images of free-form SeNPs loaded with antibiotic (Amp-SeNPs)

Fig. 6 shows the outer surface of the free nanoparticles of the nanocomposite, where the roughness coefficient (Sa) Arithmetical mean height of the surface of the free secondary compound was 1.85768 nm. When the antibiotic (Amp-SeNPs) was loaded, this measured coefficient became 3.16036 nm (Fig. 7). That is, the difference before and after loading was 1.30268 nm. This is an important criterion for increasing the effectiveness of the prepared compound, meaning that the size of the molecule loaded onto the nano surfaces plays an important role in the surface roughness, its regular crystal system, and also surface homogeneity. The results in Fig. 6 show that the root mean square height (Sq) of the nanocomposite (SeNPs) recorded 2.23558 nm, while Fig. 7 shows that the root mean square height of the antibiotic-loaded nanocomposite (Amp-SeNPs) was 4.48390 nm. The difference in root mean square height before and after loading is 2.24832 nm. The greater this difference, the greater the increase in the resulting crystal structure after loading compared to before loading [14,19]. The surface shape of the nanocomposite particles was almost homogeneous in terms of the number of protrusions above and below the surface plane (Ssk degree roughness shape), as it recorded an average of 0.0588357 (Fig. 6), which is close to 1. This indicates the homogeneity and stability of the compound. The current study showed that loading with the antibiotic reduces homogeneity, as it indicates that the compound

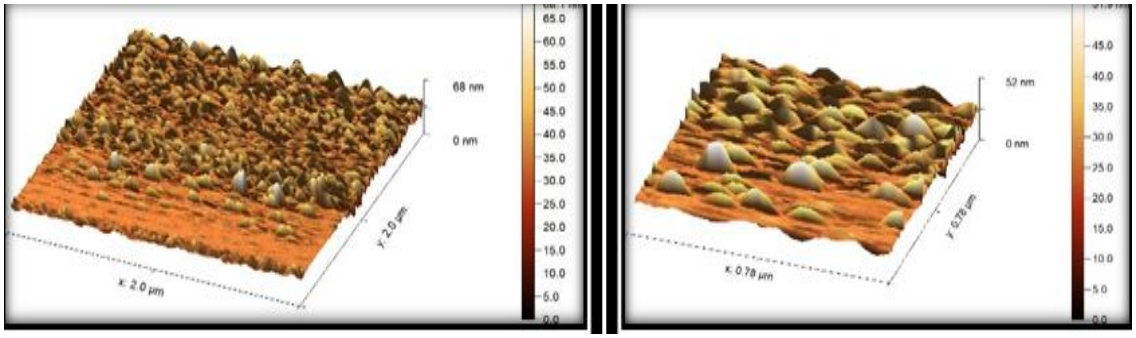

Fig. 8. Atomic Force Microscope Image of the (SeNPs) Nanocomposite showing the highest peak height and surface shape after loading with the antibiotic (AMP).

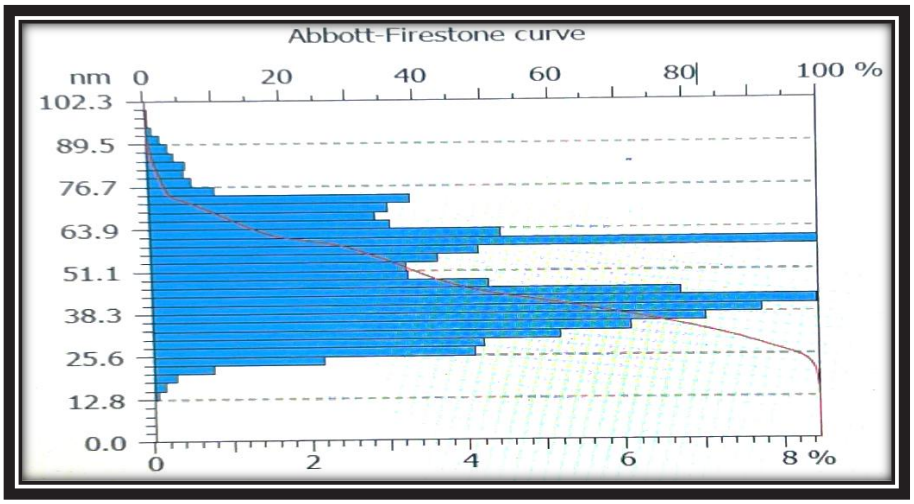

Fig. 9. Shows the particle size distribution of the nanocomposite (SeNPs) after loading with the antibiotic (AMP).

was loaded with the antibiotic even after performing the washing process several times with the activate Win centrifuge, as it showed that (Ssk) recorded an average of 0.0775372 (Fig. 6), which gives a clear idea that the distribution of particles did not apply equally to the surface plane of the compound [20,14]. The increase in reflected light intensity at the surface points of the nanocomposite, which reached 11.5, is evident in Fig. 6, where the surface appears lighter in most areas compared to the surface after loading with the antibiotic (1.68). Fig. 7 illustrates the surface shape and the increase in the projecting peaks and light-reflecting points, resulting in a darker surface compared to the surface before loading. The current results also indicate loading, as measured by the increase in the height of the projecting peaks from 10.7869 nm to 33.6400 nm, and the increase in the crater height from 7.4088 nm to 34.4935 nm. This suggests uniform loading, as evidenced by the symmetrical coverage of the surface between the peaks and their heights, as well as the increased crater height, as shown in Figs. 8, 9. The results of the study showed that the average molecular size of the nanocomposite before loading was around 106 nm, while after loading it with the antibiotic AMP it became around 118 nm.

Scanning electron microscope (SEM) images of free nanocomposite (SeNPs) and antibiotic-loaded (Amp-SeNPs)

The study showed that scanning electron microscopy (SEM) provides a clear view of the surface morphology and external geometric shape of the particles. Consequently, the prepared particles appear green, mostly in a uniform spherical shape, as in Fig. 10 before loading, where it recorded 261.2 nm, while in Fig. 11 after loading it recorded 373.3 nm. This indicates that the nanocomposite loaded with the antibody

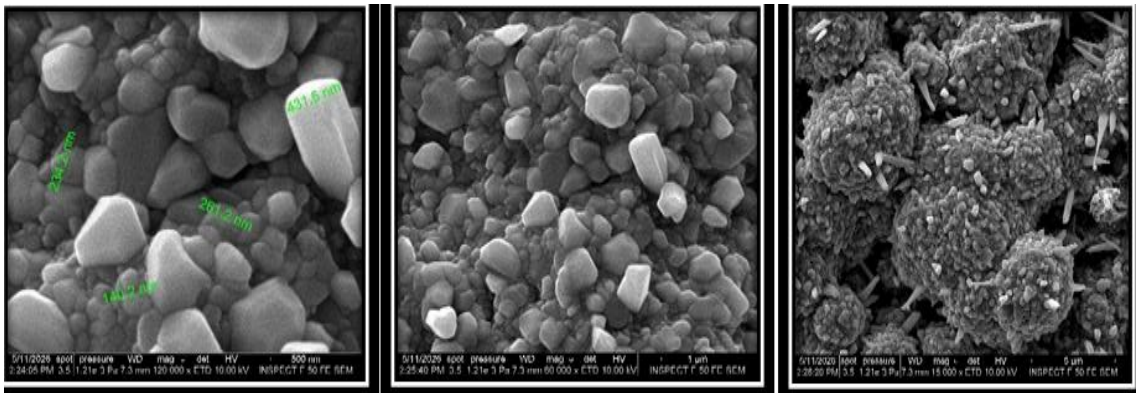

Fig. 10. Scanning electron microscope image of the nanocomposite (SeNPs) showing the geometric shape of the surface before loading with the antibiotic (AMP).

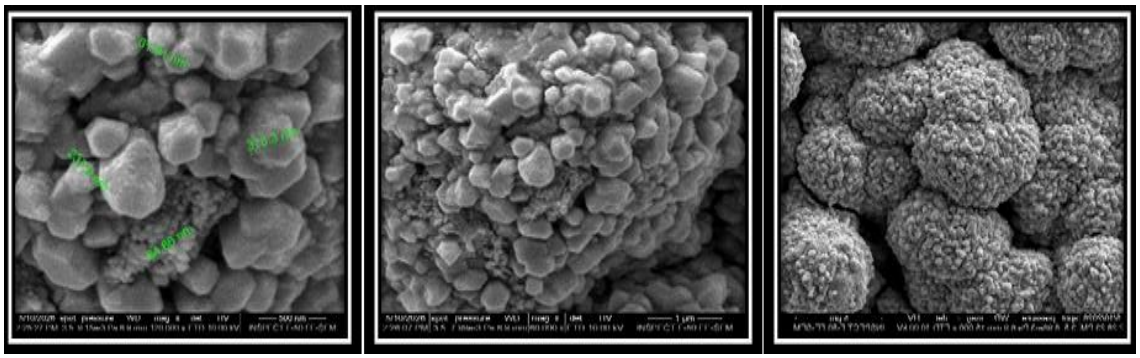

Fig. 11. Scanning electron microscope image of the nanocomposite (SeNPs) showing the geometric shape of the surface of the nanocomposite after loading with the antibiotic (AMP).

gave very high activity within a specific nanoscale range, as the results of the study were consistent with other studies that gave the same results [15].

The inhibitory effect of selenium nanoparticles (SeNPs) before and after loading with the antibiotic Ampicillin in bacteria E. coli, Klebsiella pneumoniae and Pseudomonas aeruginosa

This study investigated the inhibitory activity of the antibiotic Ampicillin before and after loading it with a nanocomposite. The synergistic inhibitory activity against both Gram-negative and Gram-positive bacteria was revealed, and the results were compared with those of Ampicillin in its free form and after loading it with the nanocomposite. The difference in inhibitory activity between the free and synergistic forms of the nanocomposite and the antibiotic was studied after calculating the minimum inhibitory concentration (MIC) for both the nanocomposite and the antibiotic under investigation.

The results of the current study on the inhibition diameter of E. coli bacteria isolated from men with prostate cancer and urinary tract infections showed significant differences in concentration levels when treated with the antimicrobial-loaded nanocomposite (Amp-SeNPs) (T3), recording (24.63 ± 1.36) mm, compared to (1.25 ± 0.366) and (11.88 ± 1.74) mm, respectively, in the (T2 and T1) treatments of free antibiotic and the nanocomposite. Table 1 also indicates that the treatment with the nanocomposite and the antibiotic (Amp-SeNPs) (T3) exhibited the highest inhibition rates at the first and second concentrations (C1 and C2). These increases in inhibition rates were significant (P≤ 0.05), reaching (24.63 ± 1.36) mm for both concentrations, compared to the rate recorded in the second treatment (T2). The concentrations recorded

Table 1. Diameter of inhibition loop (mm) when treated with the SeNPs nanocomposite before and after loading the antibiotic AMP into E. coli bacteria at two concentrations the first MIC> (C1) and the second MIC= (C2).

LSD	Average ± Standard Deviation	Concentrations	transaction
2.54	0.05±0.29	50ml/(32mg) C1	T1(AMP)
2.54	2.00±0.41	50ml/(64mg) C2	
1.79	1.25±0.366	Total	SeNPs)(T2
	7.25±0.48	50ml/(64mg) C1	
	16.50±1.32	50ml/(128mg) C2	
	11.88±1.74	Total	T3(Amp-SeNPs)
	21.75±1.11	C1)32mg/16mg(50ml/	
	27.50±0.96	C2)64mg/32mg(50ml/	
	24.63±1.36	Total	

Table 2. Diameter of inhibition loop (mm) when treated with the SeNPs nanocomposite before and after loading the antibiotic AMP into K. pneumoniae bacteria at two concentrations the first MIC> (C1) and the second MIC =(C2).

LSD	Average ± Standard Deviation	Concentrations	transaction
2.88	0.25±0.025	50ml/(32mg) C1	(AMP) T1
2.88	2.00±0.41	50ml/(64mg) C2	
2.04	1.125±0.398	Total	SeNPs)(T2
	7.00±1.080	50ml/(64mg) C1	
	14.00±1.29	50ml/(128mg) C2	
	10.500±1.535	Total	T3(Amp-SeNPs)
	20.00±1.47	C1)32mg/16mg(50ml/	
	27.75±1.258	C2)64mg/32mg(50ml/	
	23.87±1.642	Total	

were (11.88±1.74) mm for the treatment with the nanocomposite (SeNPs). The inhibition rates for all samples were higher at the second concentration for both the nanocomposite (16.50±1.32) and the antibody-loaded nanocomposite (Amp-SeNPs), reaching (27.50±0.96) mm compared to the inhibition rates recorded in all groups at the same concentration. It was found that the average diameter of inhibition in the treatment C1/T3 (21.75±1.11) mm was higher than in the treatment with the second concentration (C2/T1), where the average diameter of inhibition was (2.00±0.41) mm. This indicates that loading the antibiotic with nanomaterials leads to an increase in the effectiveness of the antibiotic and breaks the resistance of bacteria within the lowest inhibitory concentration (MIC), and increases their sensitivity to the antibiotic after they had severe resistance. As indicated by the results in Table 2, the inhibition diameter of Klebsiella pneumoniae bacteria isolated from patients showed significant differences in concentration levels when treated with the antimicrobial-loaded nanocomposite (Amp-SeNPs) (T3). The inhibition diameter recorded was (23.87 ± 1.642) mm compared to treatments T1 and T2 (1.125 ± 0.398 and 10.500 ± 1.535) mm, respectively. Treatment with the nanocomposite and the antimicrobial (Amp-SeNPs) (T3) exhibited the highest inhibition rate at both concentrations (C1 and C2). These increases in inhibition rate were significant (P≤ 0.05), reaching (23.87 ± 1.642) mm for both concentrations, compared to the rate recorded in treatment T2. The concentrations recorded were (10.500 ± 1.535) mm for the treatment with the nanocomposite (SeNPs). The inhibition rates for all samples were higher at the second concentration for both the nanocomposite (14.00 ± 1.29) and the antibiotic-loaded nanocomposite (Amp-SeNPs), which reached (27.75 ± 1.258) mm, compared to the inhibition rates recorded in all groups at the same concentration. The comparison between the

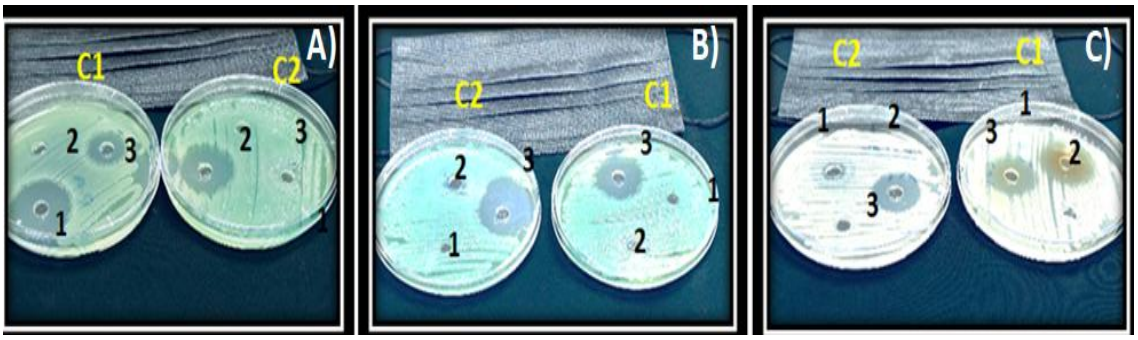

Fig. 12. Shows the inhibitory effect of the nanocomposite and the antibiotic AMP, both its free and synergistic forms, before and after loading in bacteria (A- E. coli bacteria, B- K. pneumoniae bacteria, C- P. aeruginosa).

Table 3. Diameter of inhibition loop (mm) when treated with the SeNPs nanocomposite before and after loading the antibiotic AMP into P. aeruginosa bacteria at two concentrations the first MIC> (C1) and the second MIC= (C2).

LSD	Average ± Standard Deviation	Concentrations	transaction
2.36	0.50±0.29	50ml/(32mg) C1	(AMP) T1
2.36	1.50±0.29	50ml/(64mg) C2	
1.67	1.00±0.32	Total	SeNPs)(T2
	7.75±0.63	50ml/(64mg) C1	
	12.75±1.25	50ml/(128mg) C2	
	10.25±1.29	Total	T3(Amp-SeNPs)
	20.00±0.91	C1)32mg/16mg(50ml/	
	27.00±0.82	C2)64mg/32mg(50ml/	
	23.50±1.47	Total	

inhibition diameter rate in the treatment C1/T3 (20.00 ± 1.47) mm was found to be higher than the treatment with the second concentration (C2/T1), in which the inhibition diameter rate was (2.00 ± 0.41) mm. This indicates that loading the antibiotic with nanomaterials leads to an increase in the effectiveness of the antibiotic and breaks the resistance of bacteria within the lowest inhibitory concentration (MIC), and increases their sensitivity to the antibiotic after they had severe resistance. The results in Table 3 indicate that the inhibition diameter of Pseudomonas aeruginosa bacteria isolated from male patients showed significant differences in concentration levels when treated with the antimicrobial-loaded nanoparticle (Amp-SeNPs) (T3), recording (23.50 ± 1.47) mm, compared to treatments (T1 and T2) of the free antibiotic and the nanoparticle, respectively (1.00 ± 0.32 and 10.25 ± 1.29) mm. Treatment with the nanoparticle and the antibiotic (Amp-SeNPs) (T3) exhibited the highest inhibition rate at the first and second concentrations (C1 and C2). These increases in inhibition rate were significant (P≤ 0.05), reaching (23.50 ± 1.47) mm for both concentrations, compared to the second treatment (T2). The concentrations (10.25 ± 1.29) mm for the treatment with the nanocomposite (SeNPs) showed that the inhibition rates for all samples were higher at the second concentration for both the nanocomposite (12.75 ± 1.25) and the antibiotic-loaded nanocomposite (Amp-SeNPs) (27.00 ± 0.82) mm, compared to the inhibition rates recorded in all groups at the same concentration. The comparison between the inhibition diameter in the C1/T3 treatment (20.00 ± 1.91) was found to be higher than the second concentration treatment (C2/T1), in which the inhibition diameter was (1.50 ± 0.29) mm. This indicates that the effectiveness of loading the antibiotic with nanomaterials leads to increased antibiotic efficacy and breaks bacterial resistance at the lowest inhibitory concentration (MIC), increasing their sensitivity to the antibiotic after they were highly resistant. The antibacterial nanocomposite was found to have antibacterial effects, particularly against bacteria that cause urinary tract infections. Studies have shown that the antibacterial nanocomposite inhibits the growth of bacteria such as Pseudomonas aeruginosa, Escherichia coli, and Klebsiella aerogenes. [21,15].

The results are consistent with a study that tested the antibiotic-loaded nanocomposite using various methods, including dilution chain assays and agar diffusion assays, on the growth of these bacteria. It demonstrated high inhibitory efficacy, and the antibiotic-loaded nanocomposite was particularly effective in inhibiting several organisms, exhibiting higher antibacterial activity compared to antibiotics used in their free forms. The results also suggest that the antibiotic-loaded nanocomposite has the potential to be used as a natural treatment for urinary tract infections [22,14]. The effect of ashwagandha-derived nanocomposites on these types of bacteria was investigated in this study. Medium-pore selenium nanoparticles with active nanoparticle sites and an antibiotic combination were synthesized. This nanocomposite demonstrated very high inhibitory activity against both Gram-positive and Gram-negative bacteria [23]. Nanoparticles can be used to eliminate the resistance of bacteria to the antibiotic ampicillin by disrupting some of their resistance genes [24]. Another study with similar results found that the synthesized compounds used chitosan secondary particles to enhance ampicillin delivery and reduce drug resistance via plasmid. The ampicillin-loaded nanoparticles showed high antagonistic activity against microbes, including ampicillin-resistant E. coli, K. pneumoniae, and P. aeruginosa [25]. These results also indicate that nanocomposites, such as those based on Selenium nanoparticles have been shown to have the ability to effectively eliminate these types of ampicillin-resistant bacteria [26]. The mechanism by which urinary tract infection-causing bacteria are inhibited by nanoparticles takes various forms, including coating the urinary tract, where they exhibit antibacterial and anti-adhesive properties, preventing bacteria from adhering to the urethral surface, especially when using catheters as shown in Fig. 12. Another approach involves using nano systems that have the ability to act as quorum-sensing inhibitors (QSIs) and cause microbial destruction, which are constructed sequentially according to the control and degree of bacterial colonization [27].

C1 - Inhibition zone / mm at the first concentration (MIC >(C1) in macros and grams per milliliter) C2 - Inhibition zone / mm at the second concentration (MIC = (C2) in macros and grams per milliliter) for these types of bacteria, where the first hole represents (AMP) and the second (SeNPs) and the third (Amp-SeNPs) for both concentrations and for these types of bacteria.

CONCLUSION

The study concluded that loading ampicillin onto green selenium nanoparticles enhanced antibiotic efficacy, improved its pharmaceutical properties, and broke bacterial resistance, offering a promising supportive treatment option for prostate cancer patients.

CONFLICT OF INTEREST

The authors declare that there is no conflict of interests regarding the publication of this manuscript.

REFERENCES

1. Chakrabarti D, Albertsen P, Adkins A, Kishan A, Murthy V, Parker C, et al. The contemporary management of prostate cancer. CA Cancer J Clin. 2025;75(6):552-586.
2. Złoch M, Sibińska E, Monedeiro F, Mišta W, Arendowski A, Fijałkowski P, et al. Adaptation of MALDI-TOF MS Technique for Tracking Changes in the Urinary Microbiome During and After Radiotherapy for Prostate Cancer. Cancer Manag Res. 2026;Volume 18:1-18.
3. Zowawi HM, Harris PNA, Roberts MJ, Tambyah PA, Schembri MA, Pezzani MD, et al. The emerging threat of multidrug-resistant Gram-negative bacteria in urology. Nature Reviews Urology. 2015;12(10):570-584.
4. Hetta HF, Ramadan YN, Al-Harbi AI, A. Ahmed E, Battah B, Abd Ellah NH, et al. Nanotechnology as a Promising Approach to Combat Multidrug Resistant Bacteria: A Comprehensive Review and Future Perspectives. Biomedicines. 2023;11(2):413.
5. Zhang T, Qi M, Wu Q, Xiang P, Tang D, Li Q. Recent research progress on the synthesis and biological effects of selenium nanoparticles. Frontiers in Nutrition. 2023;10.
6. Kirubakaran D, Wahid JBA, Karmegam N, Jeevika R, Sellapillai L, Rajkumar M, et al. A Comprehensive Review on the Green Synthesis of Nanoparticles: Advancements in Biomedical and Environmental Applications. Biomedical Materials and Devices. 2025;4(1):388-413.
7. AlQurashi DM, AlQurashi TF, Alam RI, Shaikh S, Tarkistani MAM. Advanced Nanoparticles in Combating Antibiotic Resistance: Current Innovations and Future Directions. Journal of Nanotheranostics. 2025;6(2):9.
8. Elshikiby LA, Baka ZAM, El-Zahed MM. Biological activities of optimized biosynthesized selenium nanoparticles using Proteus mirabilis PQ350419 alone or combined with chitosan and ampicillin against common multidrug-resistant bacteria. Microbial Cell Factories. 2025;24(1).
9. Chen YB, Hochstedler B, Pham TT, Alvarez MA, Mueller ER, Wolfe AJ. The Urethral Microbiota: A Missing Link in the Female Urinary Microbiota. J Urol. 2020;204(2):303-309.
10. Youssef MA, Hamza NM, Hussain KAM. The effect of aqueous extract of Cinnamonum zeylanicum on some biochemical parameters in male white rats in which rheumatoid arthritis is induced. AIP Conference Proceedings: AIP Publishing; 2023. p. 020031.
11. Al-Karawi RH, Al-Safy AH, Hussain KAM. Evaluation of the biological efficacy of green moringa nanocomposite in pregnant female rats treated with ibuprofen. AIP Conference Proceedings: AIP Publishing; 2026. p. 030051.
12. Shaheen AA, M. Hussain KA, Al-Safy AH. Preparation and characterization of nanocomposite from fresh green Asparagus Officinalis L. Stems and study of its biological efficacy in treating polycystic ovary syndrome induced by metformin suppository. ASEAN Journal of Psychiatry. 2024:01-09.
13. Alagesan V, Venugopal S. Green Synthesis of Selenium Nanoparticle Using Leaves Extract of Withania somnifera and Its Biological Applications and Photocatalytic Activities. BioNanoScience. 2018;9(1):105-116.
14. Al-Karawi RH, Al-Safy AH, Hussain KAM. Study the Effect of Ibuprofen Loaded with Green Nanocomposite on Blastocyst Implantation in Female Albino Rats. Lecture Notes in Networks and Systems: Springer Nature Singapore; 2025. p. 531-547.
15. Hussain KAM, Al-Rubaiy SSH, Al-awad HAR. Green synthesis and characterization of a nanocomposite Petroselinum crispum (PcNps) and evaluation of its effect on the inhibition of Pseudomonas aeruginosa before and after loading the antibiotic erythromycin. Journal of Applied and Natural Science. 2025;17(2):574-581.
16. Chaturvedi A, Ranjan R. Antimicrobial nanoparticles: a new horizon to combat multidrug-resistant bacteria. Frontiers in Nanotechnology. 2025;7.
17. Shneen SY, Hussain MIJKAM. Green Biosynthesis of Silver Nanoparticles from Moringa oleifera Leaf Extracts and Their Efficacy Against the Pulse Beetle, Callosobruchus maculatus. BIOPESTICIDES INTERNATIONAL. 2024;20(01):83.
18. Weinstein MP, Lewis JS. The Clinical and Laboratory Standards Institute Subcommittee on Antimicrobial Susceptibility Testing: Background, Organization, Functions, and Processes. J Clin Microbiol. 2020;58(3).
19. Caratelli V, Di Meo E, Colozza N, Fabiani L, Fiore L, Moscone D, et al. Nanomaterials and paper-based electrochemical devices: merging strategies for fostering sustainable detection of biomarkers. Journal of Materials Chemistry B. 2022;10(44):9021-9039.
20. Vicaș LG, Marian NA, Ali DH, Duteanu N, Svera P, Dehelean C, et al. Potentiation of the Pharmacological Effects of an Aristolochia clematitis L. Extract by Loading into Liposomes Facilitating Release to HaCaT Cells. Pharmaceutics. 2026;18(1):89.
21. Patra D, Ghosh S, Mukherjee S, Acharya Y, Mukherjee R, Haldar J. Antimicrobial nanocomposite coatings for rapid intervention against catheter-associated urinary tract infections. Nanoscale. 2024;16(23):11109-11125.
22. Traub WH, Spohr M. Fosfomycin: Interpretation of Inhibition Zones Obtained with the Bauer-Kirby Agar Disk Diffusion Susceptibility Test. Chemotherapy. 2009:208-212.
23. Hiba TS, Zainab FM. Antibacterial activity of Green Synthesis of Silver Nanoparticles from Withania Somnifera (Ashwagandha) Root Extract. Medico Legal Update. 2021;21(2):625-631.
24. Wan F, Draz MS, Gu M, Yu W, Ruan Z, Luo Q. Novel Strategy to Combat Antibiotic Resistance: A Sight into the Combination of CRISPR/Cas9 and Nanoparticles. Pharmaceutics. 2021;13(3):352.
25. Vassallo A, Silletti MF, Faraone I, Milella L. Nanoparticulate Antibiotic Systems as Antibacterial Agents and Antibiotic Delivery Platforms to Fight Infections. Journal of Nanomaterials. 2020;2020:1-31.
26. Wang Z, Zhang P, Ding X, Wang J, Sun Y, Yin C, et al. Co-delivery of ampicillin and β-lactamase inhibitor by selenium nanocomposite to achieve synergistic anti-infective efficiency through overcoming multidrug resistance. Chem Eng J. 2021;414:128908.
27. Kumar A, Kumar A, Islam MM, Borgohain R, Raikwar S. Modern Solutions to UTIs: The Role of Nanotechnology and Herbal Treatments. Curr Drug Targets. 2025;26(12):828-849.